

Fabrication and Characterization of Flower-like Zinc Oxide for Dye-Sensitized Solar Cell Photoanode

H. ABDULLAH¹, N.P. ARIYANTO¹, B. YULIARTO², S. JUNAIDI³, YAP CHI CHIN⁴, MUHAMAD YAHAYA⁴, S. SHAARI⁵

¹Department of Electrical, Electrics and Systems Engineering
University Kebangsaan Malaysia, 43600 Bangi, Selangor
MALAYSIA

²Department of Engineering Physics
Bandung Institute of Technology
INDONESIA

³Department of Mechanical and Material Engineering
University Kebangsaan Malaysia, 43600 Bangi, Selangor
MALAYSIA

⁴School of Applied Physics
University Kebangsaan Malaysia, 43600 Bangi, Selangor
MALAYSIA

⁵Institute of Microengineering and Nanoelectronic
University Kebangsaan Malaysia, 43600 Bangi, Selangor
MALAYSIA

Email: huda@vlsi.eng.ukm.my

Abstract: - Zinc oxide porous film consists of nanoparticles which assemble forming flake-like particle is synthesised through pyrolytic of chemical bath deposition product. Zinc oxide film consists of nanoparticle around 20 nm with surface area of 58.6 m²/gram is obtained in this work. Fabricated dye-sensitized solar cell (DSC) shows 1.56 % conversion efficiency with 0.44 V open-circuit voltage (V_{oc}) and 7.19 mA/cm² short-circuit current (J_{sc}). Impedance spectroscopy of the cell is fitted based on equivalent circuit describing electron transport and recombination.

Key-Words: - zinc carbonate hydroxide, zinc oxide, chemical bath deposition, nanoparticle, dye sensitized solar cell, porous film

1 Introduction

Nano-scale porous zinc oxide with high surface area have been studied to enhance physicochemical and electrochemical properties of certain applications such as gas sensor [1], photocatalyst [2] and dye-sensitized solar cell (DSC) photoanode [3].

Manipulation of zinc oxide nanostructure to be various structures such as prismatic [4], needle-like [5], tetrapods [6,7], nanorods [8,9], nanobelts [10], nanotubes [11], nanocombs [12,13] by various physical and chemical techniques leads different properties of zinc oxide. Chemical bath deposition (CBD) is used to deposit dense films of metal chalcogenides or metal oxides by single immersion of substrates in aqueous metal solutions [14]. Film deposition under CBD is affected by concentration,

temperature, pH and selecting proper and adequate quantities of additives [15,16]

Instead of dense film, fabrication of zinc oxide porous film by CBD is the objective of this work. Large surface area of zinc oxide film is preferred as important factor for DSC photovoltaic performance. Further, the DSC mechanism is studied by impedance spectroscopy to describe transport, accumulation and recombination of electron in the semiconductor phase of the cell based on impedance model of DSC equivalent circuit [17].

2 Experimental Details

Bath solutions were synthesized by dissolving zinc nitrate hexahydrate (Analytical Reagent grade from

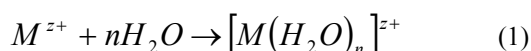
Bendosen) and urea (purity $\geq 99\%$ From Fluka) in DI water. This experiment used 0.05 M and 1.0 M of initial concentration of zinc nitrate and urea respectively. Nitric acid was added to adjust pH solution to pH~4. Clean FTO substrates, cleaned under ultrasonic in acetone, methanol and isopropyl alcohol, were put inside close container in constant oven. Sample of CBD60 and CBD80 were deposited for 24 hours at 60 °C and 80 °C respectively. As deposited films were washed by DI water and dried before heat treatment. Calcination was conducted at 300 °C and 500 °C for 30 minutes with 20 °C/minute heating rate under air ambience.

Photoanode of dye-sensitised solar cell was prepared by immersing zinc oxide film in 0.5 mM N719 ethanolic dye solutions for 30 minutes at room temperature. The dyed films then immersed in absolute ethanol for one hour to remove any aggregation which may occurred under dye immersion. Drying was sequentially conducted in oven at 55°C for at least 3 hours, followed by sandwich-like cell assembly. Liquid electrolyte of MPN-100 (Solaronix) was filled in into cell afterwards.

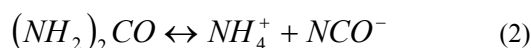
Crystallinity of deposited films were characterized by Siemens D-5000 X-ray Diffractometer. Sample morphology was observed by Zeis Supra 55VP Scanning Electron Microscope. Films surface area was measured using BET flow procedure by AMI-200 from Altamira Instrument. Oriol 150 Watt Solar simulator with 1.5 AM filter was used as light source for measurement of photovoltaic performance. Cell active area was determined using masking of 0.5 x 0.5 cm. Impedance data was obtained using Gamry Potentiostat Series G300 under illumination of Osram 50 W Halogen lamp. Measurement was conducted without current flow in frequency range from 100 KHz to 10 mHz. Fitting and analysis was conducted using Gamry Echem Analyst v.5.60.

3 Results and Discussion

In pure water, transition metal cations which is introduced as metal salts, are solvated by water molecule, forming aqua ions [18]. Dissolution of zinc nitrate hexahydrate in aqueous solutions results Zn^{2+} ions which is solvated by water molecule. Zinc ion has a solvation number of six and forms an octahedral inner coordination sphere of $[Zn(H_2O)_6]^{2+}$ [19].



Dissolved urea in solutions decomposes instantly as solutions were heated. Urea decomposition yields ammonium and carbonate ions. Carbonate ions act to regulate pH in aqueous solution by slowly supplying hydroxyl ions which increase pH value slightly. In CBD solutions, some of carbonate ions are bonded by solvated zinc ions before hydrolyses water molecule. Because of limited free of carbonate ions, hydrolysis is reduced and pH increase is repressed. As experiment data, pH solution increase from pH~4 up to pH~8.5.



Attached carbonate ions on nuclei results a carbonate compound of deposited films as shown in crystalline structure. Compared with PDF No 01-72-1100 as reference, diffraction pattern of deposited sample refers to zinc carbonate hydroxide. Calcined film at 300°C shows conversion of zinc carbonate hydroxide to be zinc oxide as shown by diffraction pattern in Fig. 1. Refers to PDF No 00-36-1451, there are two dominant peaks represent (100) and (101) plane. Crystalline size of calcined sample is calculated has value 14.1 nm and 12.6 nm for (100) and (101) plane respectively.

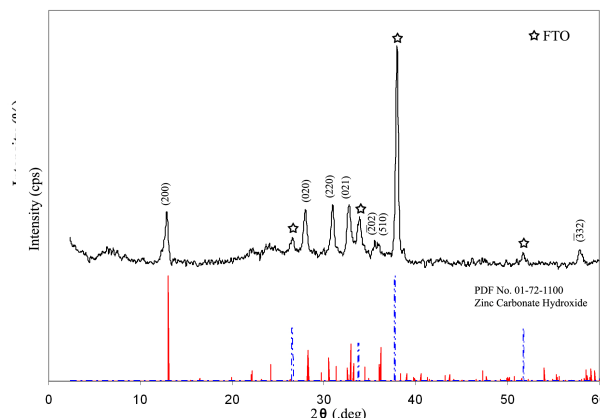


Fig. 1 Diffraction pattern of calcined sample and reference pattern of zinc oxide.

Morphology observation of calcined sample shows that flake-like structure is kept under calcination process as shown in Fig. 2. Morphology of calcined sample shows a flower like morphology. Thickness of deposited film or flower-like structure is measured around 15µm. Flower-like structure is assembled by many less than 100 nm thickness of

flake-like particles. TEM observation shows that nanoparticle with size range 10 nm up to 30 nm is composed of the flake-like particle.

Nanoparticle size of 20 nm is obtained by calcination at 300°C. Higher calcination at 500°C results bigger nanoparticle of 35 nm. SEM micrographs also show that nanoparticle aggregation occurs severely as rough surface of flake-like secondary particle.

Particle size increments reduces sample surface

area which measured by BET flow procedure. As-deposited sample only has 25.7 m²/gram surface area. Calcination process converts zinc carbonate into zinc oxide nanoparticle with surface area 58.6 m²/gram and 48.5 m²/gram for calcination at 300°C and 500°C respectively. It is shown that decomposition of carbonate leads to defects and forms zinc oxide nanoparticle. Higher calcination leads to sintering effect as the nanoparticle is compacted.

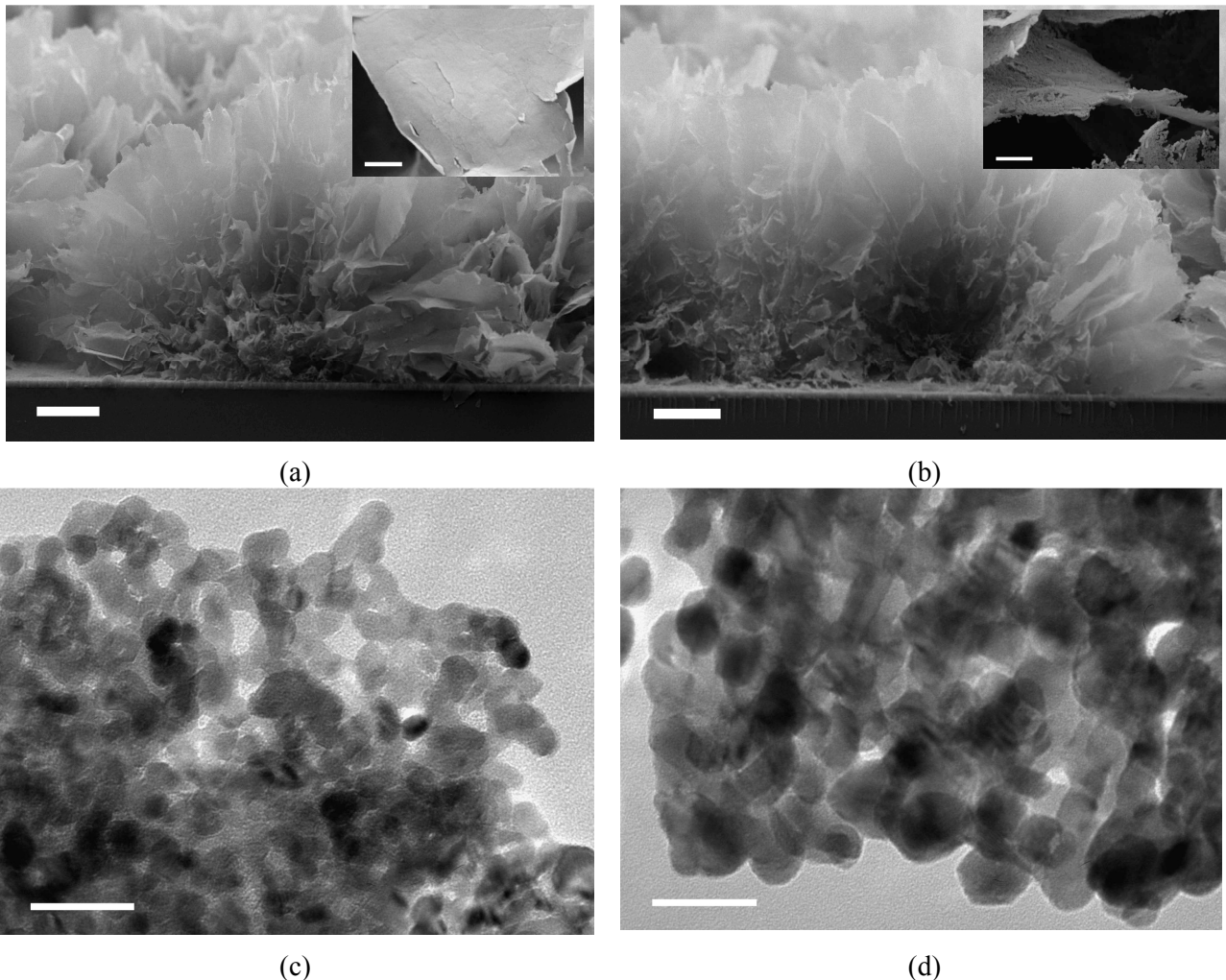


Fig. 2 SEM micrographs of calcined CBD60 sample at (a) 300°C and (b) 500°C. Scale bar is 5μm and scale bar of inset is 500 nm. TEM micrographs of calcined CBD60 sample at (c) 300°C and (d) 500°C. Scale bar is 50 nm.

Table 1. Surface area of zinc oxide films.

Sample	Surface Area (m ² /gram)
As deposited films	25.7
Calcined films at 300°C	58.6
Calcined films at 500°C	48.5

Table 2. Photovoltaic performance of fabricated DSC.

Sample	J_{SC} (mA/cm ²)	V_{OC} (V)	FF	η (%)
CBD60	1.25	0.42	0.25	0.13
CBD80	7.19	0.44	0.49	1.56

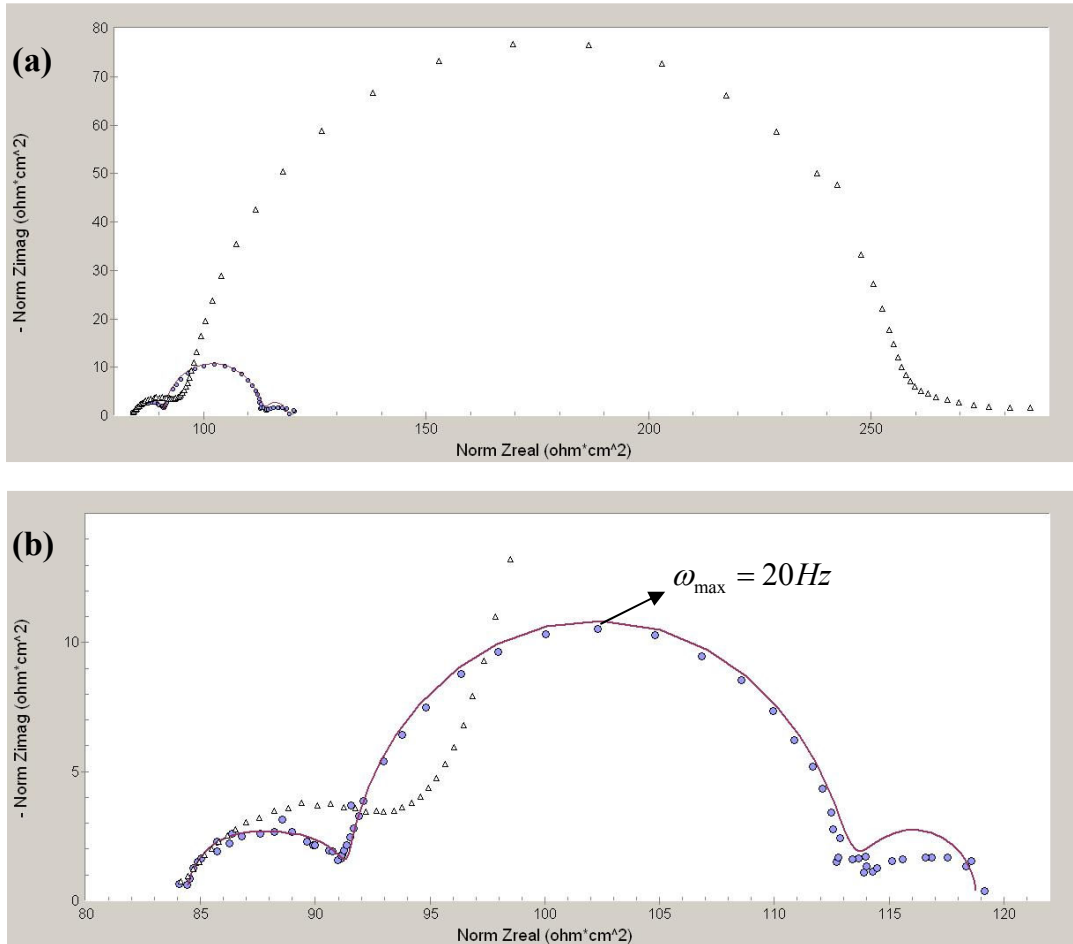


Fig. 3 (a) Nyquist plot of impedance spectrum and fitted plot between 100 KHz and 10 mHz under (Δ) dark and (●) illumination. (b) Fitted Nyquist plot of illuminated sample. Line (-) represents fitting result.

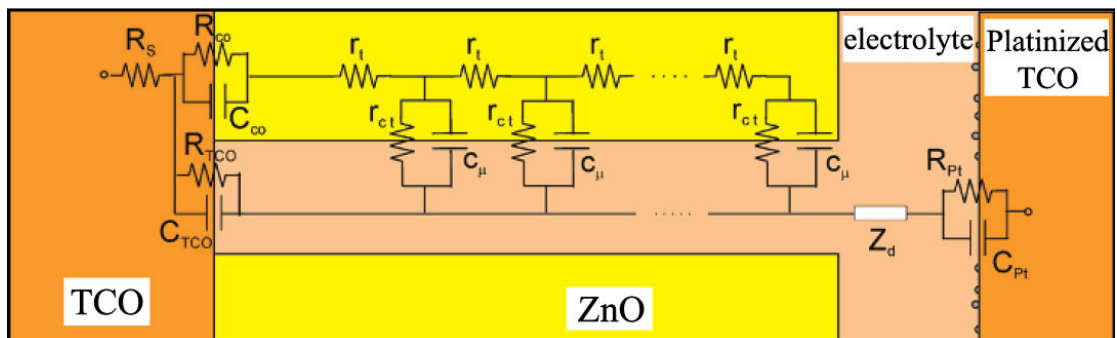


Fig. 4 Equivalent circuit model of dye-sensitized solar cell.

Photovoltaic performance of the cells, as shown on Table 2, shows that CBD80 has better performance than CBD60. CBD80 has higher particle density than CBD60, allows the cell to facilitate more adsorbed dye on its surface.

Data points of impedance spectroscopy is fitted based on equivalent circuit model of DSC shown in Fig. 4 which r_{ct} represents charge-transfer resistance of charge recombination between electron in mesoscopic semiconductor film and I_3^- in liquid electrolyte, c_μ represents chemical capacitance of mesoscopic semiconductor film, r_t represents transport resistance of nanoparticle semiconductor, Z_d represent Warburg element showing diffusion of I_3^- in electrolyte, R_{pt} and C_{pt} represent charge-transfer resistance and double-layer capacitance on counter electrode, R_{TCO} and C_{TCO} represent charge-transfer resistance and double-layer capacitance of exposed TCO|electrolyte interface, R_{CO} and C_{CO} represent resistance and capacitance at zinc oxide|TCO contact and R_s represent sheet resistance of conducting substrate [20].

Electron lifetime (τ_{eff}) in mesoscopic semiconductor, the effective electron diffusion coefficient in semiconductor film (D_{eff}) and effective electron diffusion length (L_n) is calculated using equations [21]

$$\tau_{eff} = \frac{1}{\omega_{max}} \quad (5)$$

$$D_{eff} = \frac{R_{ct} L^2}{R_t \tau_{eff}} \quad (6)$$

$$L_n = L \sqrt{\frac{R_{ct}}{R_t}} \quad (7)$$

Zinc oxide film with thickness approximately 25 μm has τ_{eff} of 50 ms and D_{eff} of $5.88 \times 10^{-4} \text{ cm}^2/\text{s}$. Calculated L_n results 54.25 μm which means optimal photoanode thickness is about 54 μm as twice as measured cell thickness.

4 Conclusion

Zinc oxide porous film from pyrolytic of CBD result shows promising photovoltaic performance as used for DSC photoanode. Electron diffusion properties with D_{eff} of $5.88 \times 10^{-4} \text{ cm}^2/\text{s}$ and L_n of 54 μm , estimated by electrochemical impedance spectroscopy lead fabricated cell can be improve for thicker semiconductor film.

Acknowledgement

This work is financially supported by The Ministry of Science, Technology and Innovation of Malaysia which under Science Fund 03-01-02-SF0386. Authors acknowledge Mr. Lukman Hakim (Fuel Cell Institute UKM) for surface area measurement.

References:

- [1] T. Wagner, et.al, *Thin Solid Films*, 515, 2007, pp. 8360-8363.
- [2] C. Hariharan, "Photocatalytic degradation of organic contaminants in water by ZnO nanoparticles: Revisited," *Applied Catalysis A: General*, 304, 2006, pp. 55-61.
- [3] K. Keis, C. Bauer, G. Boschloo, A. Hagfeldt, K. Westermark, H. Rensmo, H. Siegbahn, "Nanostructured ZnO electrodes for dye-sensitized solar cell applications," *Journal of Photochemistry and Photobiology A: Chemistry*, 148, 2002, pp. 57-64.
- [4] C.C. Lin, K.H. Liu and S.Y. Chen, "Growth and characterization of Zn-ZnO core-shell polygon prismatic nanocrystals on Si," *Journal of Crystal Growth*, 269, 2004, pp. 425-431.
- [5] R.A. McBride, J.M. Kelly and D.E. McCormack, "Growth of well-defined ZnO microparticles by hydroxide ion hydrolysis of zinc salts," *Journal of Materials Chemistry*, 13, 2003, pp. 1196-1201.
- [6] M.C. Newton and P.A. Warburton, "ZnO tetrapod nanocrystals," *Material Today*, Vol. 10, No. 5, 2007, pp. 50-54.
- [7] M.C. Newton, S. Firth, T. Matsumura and P.A. Warburton, "Synthesis and characterization of zinc oxide tetrapod nanocrystals," *Journal of Physics: Conference Series*, 26, 2006, pp. 251-255.
- [8] X.L. Hu, Y.J. Zhu and S.W. Wang, "Sonochemical and microwave-assisted synthesis of linked single-crystalline ZnO rods," *Material Chemistry and Physics*, 88, 2004, pp. 421-426.
- [9] W.D. Zhou, X. Wu, Y.C. Zhang and M. Zhang, "Solvothermal synthesis of hexagonal ZnO nanorods and their photoluminescence properties" *Materials Letters*, 61, 2007, pp. 2054-2057.
- [10] J. Zhang, W. Yu and L. Zhang, "Fabrication of semiconducting ZnO nanobelts using halide source and their photoluminescence properties," *Physics Letters A*, 299, 2002, pp. 276-281.
- [11] R.M. Wang, Y.J. Xing, J. Xu and D.P. Yu, "Fabrication and microstructure analysis on

- zinc oxide nanotubes,” *New Journal of Physics*, 5, 2003, pp. 115.1-115.7.
- [12] C.X. Xu, X.W. Sun, Z.L. Dong and M.B. Yu, “Self-organized nanocomb of ZnO fabricated by Au-catalyzed vapor-phase transport,” *Journal of Crystal Growth*, 270, 2004, pp. 498-504.
- [13] Y.S. Lim, J.W. Park, S.T. Hong and J. Kim, “Carbothermal synthesis of ZnO nanocomb structure,” *Materials Science and Engineering B*, 129, 2006, pp. 100-103.
- [14] K. Kakiuchi, E. Hosono, T. Kimura, H. Imai and S. Fujihara, “Fabrication of mesoporous ZnO nanosheet from precursor template grown in aqueous solutions,” *Journal of Sol-Gel Science Technology*, 39, 2006, pp. 63-72.
- [15] K. Govender, D.S. Boyle, P.B. Kenway and P. O’Brien, “Understanding the factors that govern the deposition and morphology of thin films of ZnO from aqueous solutions,” *Journal of Material Chemistry*, 14, 2004, pp 2575-2591.
- [16] Z.L. Wang, Y. Liu and Z. Zhang, *Handbook of Nanophase and Nanostructured Materials Vol.1*, Kluwer Academic/Plenum Publishers, 2003.
- [17] F.F. Santiago, J. Bisquert, G.G. Belmonte, G. Boschloo and A. Hagfeldt, “Influence of electrolyte in transport and recombination in dye-sensitized solar cells studied by impedance spectroscopy,” *Solar Energy Materials & Solar Cells*, 87, 2005, pp. 117 – 131.
- [18] C.J. Binker & G.W. Scherer, *Sol Gel Science: The Physics and Chemistry of Sol-Gel Processing*, London: Academic Press, Inc., 1990.
- [19] E. Hosono, S. Fujihara, T. Kimurka and H. Imai, “Non-basic solution routes to prepare ZnO nanoparticles,” *Journal of Sol-Gel Science and Technology*, 29, 2004, pp. 71 – 79.
- [20] F.F. Santiago, J. Bisquert, E. Palomares, L. Otero, D. Kuang, S.M. Zakeerudin and M. Gratzel, “Correlation between photovoltaic performance and impedance spectroscopy of dye-sensitized solar cells based on ionic liquid,” *Journal of Physical Chemistry C*, 111, 2007, pp. 6550 – 6560.
- [21] W.H. Chiu, C.H. Lee, H.M. Cheng, H.F. Lin, S.C. Liao, J.M. Wu and W.F. Hsieh, “Efficient electron transport in tetrapod-like ZnO metal-free dye-sensitized solar cells,” *Energy & Environmental Science*, 2, 2009, pp. 694 – 698.